DMD Fast Forward. Published on September 23, 2005 as doi:10.1124/dmd.105.004010
This article has not been copyedited and formatted. The final version may differ from this version.

SPECIES DIFFERENCES IN THE ELIMINATION OF A PPAR AGONIST HIGHLIGHTED BY OXIDATIVE METABOLISM OF ITS ACYL GLUCURONIDE

Christopher J. Kochansky, Yuan-Qing Xia, Sui Wang, Brian Cato, Mellissa Creighton, Stella H. Vincent, Ronald B. Franklin, and James R. Reed

Department of Drug Metabolism, Merck Research Laboratories, Rahway, NJ 07065, (C.J.K., Y-Q.X., S.W., B.C., M.C., S.H.V., R.B.F., and J.R.R.)

RUNNING TITLE PAGE

a)Running title: OXIDATIVE METABOLISM OF AN ACYL GLUCURONIDE

b)Corresponding author: Christopher Kochansky, Merck Research Laboratories, P.O. Box 4 Sumneytown Pike, WP75B-2308, West Point, PA, USA 19486
Phone: (215) 652-9391 Fax: (215) 993-1245
Christopher_Kochansky@merck.com

c) Text pages: 30
Tables: 3
Figures: 9
References: 18
Abstract: 215 words
Introduction: 301 words
Discussion: 892 words

d) Abbreviations: MRL-C, 2-[[5,7-dipropyl-3-(trifluoromethyl)-1,2-benzisoxazol-6-yl]oxy]-2-methylpropanoic acid; PPAR, peroxisome proliferator activated receptor; CYP, cytochrome P450; UGT, uridine diphosphoglucuronosyl transferase; HPLC, high performance liquid chromatography; LC-MS/MS, liquid chromatography tandem mass spectrometry; IDA, information-dependent-acquisition; NADP and NADPH, nicotinamide adenine dinucleotide phosphate and reduced form, respectively; UDPGA, uridine 5′-diphosphoglucuronic acid

ABSTRACT

A species difference was observed in the excretion pathway of (2-[[5,7-dipropyl-3-(trifluoromethyl)-1,2-benzisoxazol-6-yl]oxy]-2-methylpropanoic acid (MRL-C), an α-weighted dual PPARα/γ agonist. Following intravenous or oral administration of [^{14}C]MRL-C to rats and dogs, radioactivity was excreted mainly into the bile as the acyl glucuronide metabolite of the parent compound. In contrast, when [^{14}C]MRL-C was administered to monkeys, radioactivity was excreted into both the bile and the urine as the acyl glucuronide metabolite, together with several oxidative metabolites and their ether or acyl glucuronides. Incubations in hepatocytes from rats, dogs, monkeys, and humans showed the formation of the acyl glucuronide of the parent compound as the major metabolite in all species. The acyl glucuronide and several hydroxylated products, some which were glucuronidated at the carboxylic acid moiety, were observed in incubations of MRL-C with NADPH- and UDPGA-fortified liver microsomes. However, metabolism was more extensive in the monkey microsomes than those from the other species. When the acyl glucuronide metabolite of MRL-C was incubated with NADPH-fortified liver microsomes, in the presence of saccharo-1,4-lactone, it underwent extensive oxidative metabolism in the monkey but considerably less in the rat, dog, and human liver microsomes. Collectively, these data suggested that the oxidative metabolism of the acyl glucuronide might have contributed to the observed in vivo species differences in the metabolism and excretion of MRL-C.

INTRODUCTION

The compound (2-[[5,7-dipropyl-3-(trifluoromethyl)-1,2-benzisoxazol-6-yl]oxy]-2-methylpropanoic acid, MRL-C; Fig. 1) is an α-weighted dual PPAR (peroxisome proliferating activated receptor) α/γ agonist (Liu et al., 2005). The PPARs are ligand-dependent transcription factors that target a group of genes involved in lipid transport and metabolism (Bishop-Bailey, 2000; Kersten et al., 2000). Upon ligand binding, the PPAR forms obligate heterodimers with the retinoic acid receptor to effect gene transcription. Three isotypes of PPAR have been identified, PPAR α, γ, and δ. PPAR α and γ have been shown to regulate genes involved in lipid catabolism and storage, respectively. PPAR γ agonists (thiazolidinediones) and PPAR α agonists (fibrates) have been used as drug therapies for type-2 diabetes and dyslipidemia, respectively (Kersten et al., 2000; Willson et al., 2001; Schoonjans et al., 1996; Wahli et al., 1995; Berger and Moller, 2002).

As reported herein, a significant species difference in the in vivo metabolism and excretion of MRL-C was observed. In rats and dogs, MRL-C was eliminated almost exclusively by acyl glucuronidation, followed by biliary excretion of the conjugate. In contrast, in monkeys, the compound was eliminated by both Phase I and Phase II metabolism, followed by excretion of the metabolites into urine and bile.

It is generally accepted that xenobiotics undergo cytochrome P450-mediated metabolism (Phase I) and then are further metabolized by a conjugation reaction such as glucuronidation (Phase II) (Parkinson, 1996). Here, evidence is presented that the acyl glucuronide of MRL-C is a substrate for Phase I metabolism by cytochrome(s) P450 in the monkey, and that the species differences observed in the metabolism and excretion of

MRL-C may be explained, in part, by differences in the oxidative metabolism of the acyl glucuronide. In vitro metabolism experiments were conducted to help elucidate the observed differences in the metabolic disposition of MRL-C in monkeys compared to rats, dogs and humans.

MATERIALS AND METHODS

Radiochemicals. [Propanoate-3-^{14}C]MRL-C, with a specific activity of 150 μCi/mg, was synthesized by the Labeled Synthesis group at the Merck Research Laboratories (Rahway, NJ). The acyl glucuronide of [^{14}C]MRL-C was isolated from bile of rats dosed orally at 2 mg/kg with [^{14}C]MRL-C at 40 μCi/mg. Briefly, bile was extracted with 3 volumes of ethyl acetate, repeated 3 times, and the extract was concentrated by evaporation under N_2. The reconstituted extract was then subjected to HPLC analysis on a Zorbax SB-phenyl column, 9.4 x 250 mm with a 5 μm particle size (Agilent Technologies, DE). The isolated acyl glucuronide was purified further using a Zorbax RX-C8, 9.4 x 250 mm with a 5 μm particle size (Agilent Technologies, DE). The purity of the acyl glucuronide was confirmed by LC-MS/MS and ^{1}H NMR analysis, which showed no evidence of rearrangement or hydrolysis.

Reagents: Liver microsomes were prepared by differential centrifugation (Raucy and Lasker, 1991). Hepatocytes were prepared from fresh male rat lives, and frozen male and female dog, monkey and human livers as described by Pang et al. (1997). Monoclonal antibodies to CYP3A and 2C enzymes in mouse ascites fluid were prepared as described by Mei et al. (1999), and provided by Dr. Magang Shou (Merck Research Labs, West Point, PA). Microsomes prepared from Baculovirus-infected cells containing individually expressed CYP isoforms and NADPH cytochrome P450 reductase were obtained from Dr. Tom Rushmore (Merck Research Labs, West Point, PA). Baculovirus/insect cell expressing human UGT1A1, 1A3, 1A4, 1A6, 1A8, 1A9, 1A10, 2B7, and 2B15 Supersomes® were purchased from BD Gentest™ (Woburn, MA).

Animal Experiments. All studies were reviewed and approved by the Merck Research Laboratories Institutional Animal Care and Use Committee with the dog and monkey studies approved and conducted by Charles River Laboratories. Doses were prepared in ethanol:50 mM Tris, pH 8.0 (20/80, v/v) for all studies, except for the biliary excretion study in rats, in which the oral (p.o.) dose was prepared in 0.5% (w/v) aqueous methylcellulose and the intravenous (i.v.) dose in ethanol:PEG400:water (10/40/50, by volume). The i.v. doses for the dog and monkey studies at 0.5 mg/kg were sterilized by filtration using a 0.22 μm filter.

Studies in Rats. [^{14}C] MRL-C (40 μCi/mg) was dosed orally (2 mg/kg, 5 ml/kg, n=2), or intravenously (1 mg/kg, 1 ml/kg, n=3) to adult male Sprague-Dawley rats (360-440 g) whose bile duct had been surgically cannulated. Bile and urine were collected up to 72 hr post dose into bottles containing 0.5 M formate buffer, pH 3 to stabilize the acyl glucuronides. Samples at 0-2 hr, 2-4 hr, 4-6 hr, and 6-8 hr samples were collected with 2 ml of formate buffer while the 8-24 hr, 24-48 hr, and 48-72 hr samples were collected with 5 ml of the buffer. The weights of acidified bile and urine collected at each time point were determined, and 100-200 μl aliquots were mixed with 7 ml Scintisafe Gel cocktail (Fisher Scientific, NJ) and counted using a 1900TR Liquid Scintillation Analyzer (Packard, CT) to estimate the radioactivity concentrations. In a separate experiment, rats were dosed with [^{14}C]MRL-C at 2 mg/kg P.O. and blood was collected by cardiac puncture from CO_2 anesthetized animals into heparinized tubes at 1, 4, 8, and 24 hr after dosing (n=2 per time point). Plasma, obtained by centrifugation (1850x g for 15min at 4°C), was acidified with 0.5 M formate buffer, pH 3.0, (0.3 ml of buffer/ml plasma) prior to freezing at -80°C.

Studies in Dogs and Monkeys. [^{14}C]MRL-C was dosed orally (2 mg/kg, 2 ml/kg) or intravenously (0.5 mg/kg, 0.5 ml/kg) to bile duct-cannulated adult male beagle dogs (10 μCi/mg, n=3/route) weighing 10 to 13 kg, and rhesus monkeys (14-17 μCi/mg, n=2/route) weighing 4 to 6 kg. Blood samples (3 ml) were collected into heparinized tubes from venipuncture of a cephalic vein of dog or a femoral vein of monkey at selected time points. Bile, urine, and feces samples were collected at selected intervals up to 5 days. Bile and urine were collected into reservoirs containing 2% aqueous formic acid, while plasma was acidified after centrifugation. The weights of acidified bile and urine collected at each time point were determined,, and concentrations of radioactivity in plasma, urine, bile and fecal homogenates were determined by combustion of weighed aliquots (0.1-0.3 g) followed by liquid scintillation counting.

In Vitro Experiments. *Hepatocytes.* [^{14}C]MRL-C (10 μM, ~13 μCi/μmol) was incubated with freshly isolated rat, dog, monkey, and human hepatocytes (10^6 cells/ml) at 37°C for up to 120 min. The reactions were stopped by the addition of one volume of acetonitrile containing 2% formic acid.

Microsomes. [^{14}C]-Labeled MRL-C (10 μM, ~13 μCi/μmol) and its acyl glucuronide (10 μM) were incubated with rat, dog, monkey, and human liver microsomes (1 mg protein/ml) with and without NADPH (1 mM) and UDPGA (5 mM). All incubations were carried out at 37°C in 0.1 M potassium phosphate at pH 7.4 in the presence of 1 mM $MgCl_2$. The NADPH was added either as a freshly prepared solution in water or as a regenerating system consisting of 10 mM glucose-6-phosphate, 1.4 units/ml of glucose-6-phosphate dehydrogenase, and 1 mM NADP. For the glucuronidation reactions, 50 μg/ml of the pore forming peptide, alamethicin (dissolved in 1:1 acetonitrile:water), was

used to enhance glucuronidation, and 5 mM saccharo-1,4-lactone (dissolved in water) was added to inhibit β-glucuronidase activity. Incubations were quenched at different time points (0-120 min) with 2/5 volume of acetonitrile containing 2% formic acid. Samples were spun in a centrifuge at 14,000 rpm for 10 min at 4°C, and 100-μl aliquots of the supernatants were analyzed by HPLC (vide infra).

Effect of Monoclonal Antibodies. Human liver microsomes (1 mg protein/ml) were preincubated with 2 μl of cytochrome P450-specific monoclonal antibody and/or control ascites fluid in 0.1 M Tris buffer at pH 7.5, together with 5 mM saccharolactone, and 2.2 units/ml of glucose-6-phosphate dehydrogenase for 30 min at room temperature. [^{14}C] MRL-C or its acyl glucuronide was added from a stock solution such that the final concentration was 10 μM. Solutions were pre-incubated for 5 min at 37^{o}C, and 30-min incubations were initiated with 10 μl of an NADPH-regenerating solution containing NADP (26 mM), glucose-6-phosphate (66 mM), and $MgCl_2$ (66 mM). The total volume of the incubation mixture was 200 μl. Reactions were stopped with 0.1 ml of acetonitrile. Samples were spun in a centrifuge at 14,000 rpm for 10 min at 4°C, and 100-μl aliquots of the supernatants were analyzed by HPLC.

Recombinant Enzymes. Incubations of the [^{14}C]-labeled acyl glucuronide with recombinant CYP2C8, 2C9, and 2C19 (200 pmol/ml) were carried out as described for incubations with liver microsomes in the presence of an NADPH-regenerating system. Incubations of [^{14}C]MRL-C with Baculovirus/insect cell expressing human UGT1A1, 1A3, 1A4, 1A6, 1A8, 1A9, 1A10, 2B7, and 2B15 Supersomes® at 0.5 mg protein/ml, were carried out for 30 min as described for incubations with liver microsomes in the presence of UDPGA.

LC-MS/MS Analysis. Identification of metabolites in samples from both in vitro and in vivo metabolism studies was achieved by on-line LC-MS/MS analysis of acetonitrile extracts. In vivo samples were prepared for analysis by first mixing 1 ml of sample with 1 ml of acetonitrile containing 0.1% formic acid. This was then spun in a centrifuge at 3000 rpm and 15°C for 15 min. The supernatant was transferred and evaporated under a steady-stream of N_2. When ready for analysis, samples were then reconstituted in mobile phase. The LC system consisted of two Perkin-Elmer series 200 pumps and a Perkin-Elmer series 200 autosampler. Radiochromatograms were obtained from the same LC runs using an on-line Flow Scintillation Analyzer (Packard, CT). Separation of metabolites was performed at room temperature on a Betasil C-18 column (250 x 4.6 mm, 5-µm from Keystone Scientific, PA). The column was eluted with a mixture of 1 mM ammonium acetate in water as mobile phase A and 1 mM ammonium acetate in methanol/acetonitrile (50/50, v/v) as mobile phase B. Elution was achieved using a linear gradient from 40 to 70% B over 10 min, followed by a 7-min hold at 70% B and a 3-min linear gradient to 90% B. The flow rate was 1 ml/min. One-fifth of the column eluate was directed into a PE SCIEX API 3000 mass spectrometer equipped with a Turbo ion-spray source, and the remaining was used for on-line radiometric detection. All radioactive waste generated was disposed of according to guidelines set by Merck Research Lab's Department of Health Physics. The mass spectrometer was operated in the negative ion mode at 400°C. Data acquisition was carried out using Analyst software (version 1.1) with built-in information-dependent-acquisition (IDA) scan function. A constant neutral loss scan of 86 Da (loss of 2-methyl propionic acid) was used as the survey scan to trigger the collection of product ion spectra for the detection of

metabolites or multiple reaction monitoring of the major transitions for metabolites was employed: MRL-C, 372/286; M16, 548/286; M15, M14, 388/302; M13, M10, 564/388; M12, M9, 386/300; M11, M8, 562/300; M7, 404/318; M6, M4, 402/316; M5, M1, 578/316; and M2, 580/318.

RESULTS

Metabolite Characterization by LC-MS/MS. The negative product-ion spectrum of MRL-C ($[M-H]^-$ at *m/z* 372) exhibited major fragments at m/z 286, 217 and 188 as shown in Fig. 1. This information was used to develop MS/MS scan experiments such as constant neutral loss of 86 Da, and multiple reaction monitoring (MRM) for metabolite transitions. However, since the metabolites were formed by hydroxylation and oxidation of the *n*-propyl side chains, followed by glucuronidation, it was not possible to assign the exact location of the biotransformation(s) based on the mass spectral data. The chemical structures depicted in Fig. 2 indicate the addition of 14, 16, 30, 32, 48 or 176 (glucuronide) daltons.

Excretion and In Vivo Metabolism. The cumulative excretion of radioactivity into urine and feces following IV and oral administration of [^{14}C] MRL-C to rats, dogs and monkeys is shown in Table 1. In rats and dogs, the majority of the radioactivity was recovered in the bile, 96 and 89%, respectively, after oral administration at 2 mg/kg. In both species, excretion of radioactivity into the urine was minimal, <1% in rats and <3% in dogs. In contrast, excretion of radioactivity in monkeys was more balanced, with 27 and 64% of the dose recovered in the bile and 42 and 24% in the urine, following p.o. and i.v. administration, respectively.

Following p.o. administration at 2 mg/kg, the major radioactive component of rat and dog plasma was parent compound (≥80%). However, parent compound only accounted for ~20% of the radioactivity in monkey plasma, which also contained several oxidative metabolites (M4, M6, M7, M9, M12, M14, and M15), their corresponding acyl glucuronides (M10 and M13) or ether glucuronides (M2), as well as the acyl glucuronide

of parent compound (M16) (data not shown). Fig. 3 illustrates the HPLC radiochromatograms of 0-72 hr pooled bile from rats, dogs, and monkeys following administration of [^{14}C]MRL-C at 2 mg/kg p.o. Similar profiles were obtained after i.v. dosing (data not shown).

The radioactive metabolite profile in pooled monkey urine is depicted in Fig. 4. Concentrations of radioactivity in rat and dog urine were insufficient for radiometric analysis and metabolite identification.

Metabolism was the primary pathway of elimination for [^{14}C]MRL-C, as the majority of excreted radioactivity was comprised of metabolites. Only trace amounts of the parent compound were observed in the bile and urine (<2% of the total radioactivity excreted). The predominant metabolite detected in rat and dog bile was the acyl glucuronide conjugate, which accounted for greater than 80% of the radioactivity, corresponding to ~77 and 71% of total dose recovered, respectively. Following i.v. and p.o. administration to monkeys, the acyl glucuronide conjugate accounted for only 18 and 37% of the radioactivity in bile, corresponding to 5 and 24% of the total dose recovered, respectively. The remainder of the radioactivity in monkey bile (20-40% of the radioactivity in bile, ~5-10% of total dose excreted) was comprised mostly of the di-hydroxylated product, M7, its ether glucuronide conjugate, M2, and the ether glucuronide M1 (Fig. 3 and 5). As shown in the radiochromatograms of Fig. 3, these metabolites were found in much lower amounts in rat and dog bile. This was also true for other oxidized products (M3, M4, M6, M9, M12, M14, and M15) and their acyl glucuronide conjugates (M5, M8, M10, M11, and M13) (Figure 3). In fact, of the five acyl glucuronide conjugates of Phase 1 metabolites, only M13 was detected in rat and dog

bile. Metabolite assignments were made using mass spectral data gathered from neutral loss-triggered data-dependent product ion scans or, as shown in Fig. 5, reconstructed ion chromatograms following multiple reaction monitoring of known metabolite transitions. Fig. 5 is a reconstructed ion chromatogram of 19 different mass transitions that are distinct for the metabolites of interest.

In monkey urine (Fig. 4), the di-hydroxylated metabolite, M7, accounted for ~50% of the radioactivity, corresponding to 20% of the total oral dose administered. The remainder of the radioactivity was distributed among the Phase 1 metabolites (M4, M6, M12, M14, and M15) and their ether (M1, M2) and acyl glucuronide conjugates (M5, M8, M10, M11, M13).

In Vitro Metabolism

Liver Microsomes and Hepatocytes. Incubation of [^{14}C]MRL-C with liver microsomes, in the presence of NADPH, resulted in a species difference with regard to the extent of metabolism. The extent of metabolism after a 30-min incubation with monkey liver microsomes was approximately 80%, compared to ~60, 43 and 20% in dog, human, and rat (Table 2). Metabolites identified in these incubations included two monohydroxylated products, (M15, major in monkey, dog and human, and M14), a ketone derivative (M12), and a di-hydroxylated product (M7) (Fig. 6).

Incubation of [^{14}C]MRL-C with hepatocytes (data not shown) and liver microsomes in the presence of UDPGA alone or with NADPH and UDPGA together (Table 2 and Fig. 7) resulted in the rapid formation of the acyl glucuronide in all species examined. Upon further incubation in the NADPH- and UDPGA-fortified liver microsomes, the acyl glucuronide disappeared gradually, resulting in the appearance of several new peaks in

the radiochromatograms. Metabolism of the acyl glucuronide was more pronounced in monkey liver microsomes than in rat, dog, or human. Results from 30-min incubations are listed in Table 2. Metabolite profiles of MRL-C incubations with monkey liver microsomes in the presence of NADPH and UDPGA at different time points are shown in Fig. 8. Metabolites in the monkey liver microsome incubations (Fig. 7 and 8) included M9, M12, M14, M15, and their acyl glucuronide conjugates (M8, M10, M11, and M13). Notably, the hydroxylated acyl glucuronide derivatives were present only at trace levels in incubations with rat, dog and human liver microsomes.

Incubation of the [^{14}C]-labeled acyl glucuronide with liver microsomes in the presence of saccharolactone and NADPH resulted in the formation of various hydroxylated products of the acyl glucuronide (M8, M10, M11, and M13) and their corresponding aglycones (M9, M12, M14 and M15). Approximately 27% of the acyl glucuronide remained after 30 min of incubation in monkey liver microsomes (Table 2 and Fig. 9), compared to 66% in dog, 83% in human, and 94% in rat (Table 2). Longer incubations resulted in increased metabolism of the acyl glucuronide in dog and monkey but not rat or human liver microsomes. In control incubations in the absence of NADPH and UDPGA, there was <5% hydrolysis of the acyl glucuronide, presumably due, in part, to the inhibition of β-glucuronidase by saccharolactone (data not shown). No re-glucuronidation was possible, since there was no UDPGA in these incubations.

Cytochrome P450 Identification. The cytochrome P450 isozyme involved in the oxidation of the acyl glucuronide in human liver microsomes was determined by incubating [^{14}C]-labeled acyl glucuronide with recombinant CYP2C8, CYP2C9 and CYP2C19, and with human liver microsomes that were pre-incubated with anti-

CYP2C8/9 and 3A4 monoclonal antibodies. The anti-CYP2C8/9 and 3A4 antibodies caused 92% and 18% inhibition of the metabolism in human liver microsomes, respectively, and when combined, inhibited all metabolism (data not shown). With recombinant CYP2C enzymes, metabolism of the acyl glucuronide was only observed upon incubation with recombinant CYP2C8, resulting in ~6% turnover following 2 hr of incubation. The results from both sets of experiments indicated that the acyl glucuronide was metabolized by CYP2C8, not CYP2C9, with some minor contribution from CYP3A4.

[^{14}C] MRL-C was incubated with human UGT1A1, 1A3, 1A4, 1A6, 1A8, 1A9, 1A10, 2B7, and 2B15 Supersomes®. The results suggested that formation of the acyl glucuronide of MRL-C could be catalyzed by several human UGT isozymes with 2B7, 1A9, and 1A3 exhibiting the highest activity (Table 3).

DISCUSSION

Following oral administration to rats and dogs, [^{14}C]MRL-C was eliminated principally as the acyl glucuronide of the parent compound, followed by its excretion into the bile. In contrast, elimination [^{14}C]MRL-C in rhesus monkeys occurred by both acyl glucuronidation and oxidative metabolism, followed by excretion of the Phase 1 and Phase 2 metabolites into the bile and urine (Figures 3-5). Most notably, several of the metabolites excreted into the monkey bile were formed by both Phase I and Phase II pathways. Similarly, monkey plasma contained several oxidative metabolites and their acyl or ether glucuronides, in addition to parent compound and its acyl glucuronide. Parent compound comprised only ~20% of radioactivity in monkey plasma at 2 and 6 hr (data not shown). By way of contrast, in rats and dogs dosed with [^{14}C]MRL-C, parent compound was the major radioactive component in plasma (≥80% of radioactivity).

Incubations of [^{14}C]MRL-C with liver microsomes, in the presence of UDPGA, (Table 2) and hepatocytes (data not shown) from rats, dogs, monkeys, and humans generated the acyl glucuronide as the major metabolite. Incubations with human UGT Supersomes® revealed that many UGT isozymes have the ability to glucuronidate MRL-C with UGT2B7, UGT1A9, and UGT1A3 displaying the highest activity towards glucuronidation of MRL-C. Under oxidative conditions, similar mono- and di-hydroxylated metabolites were formed by liver microsomes from all species, although there appears to be a species difference in the rate of metabolism. Thus, oxidative metabolism was greatest in monkey liver microsomes followed by dog > human > rat (Table 2 and Fig. 6). Incubations of [^{14}C] MRL-C in the presence of both UDPGA and NADPH resulted in a greater production of glucuronides of oxidative metabolites in

monkey, in addition to the acyl glucuronide, although the extent of overall metabolism of parent compound was similar in all species (Table 2 and Fig. 7). Even though Phase I metabolism in the monkey was greater than in the dog and much greater than in the rat, this observation did not fully explain the in vivo data, which showed a wider spectrum of metabolites (especially hydroxylated acyl glucuronides) in the monkeys. Thus, it was hypothesized that Phase I metabolism of the major metabolite, the acyl glucuronide, may have contributed to the discrepancies between the in vitro and in vivo metabolite profiles.

The speculation that some of the oxidized acyl glucuronide derivatives (M8, M10, M11, and M13) could have been formed by oxidation of the acyl glucuronide was supported through in vitro generation via incubation of [^{14}C]-labeled acyl glucuronide with NADPH-fortified liver microsomes (Fig. 9). In the in vitro incubations, these metabolites could only have been formed by oxidation of the acyl glucuronide since UDPGA was not present in the incubation. It is unlikely that the metabolites were formed from hydrolysis of the acyl glucuronide, subsequent oxidation of [^{14}C] MRL-C, and re-conjugation with glucuronic acid via endogenous UDPGA, since the [^{14}C]-labeled acyl glucuronide was shown to be stable in incubations with monkey liver microsomes and saccharolactone (in the absence of NADPH and UDPGA); less than 5% de-conjugation to the parent compound was observed after 2 hr of incubation (data not shown). Moreover, comparison of metabolite profiles from incubations of the acyl glucuronide with NADPH and those of MRL-C in the presence of NADPH-fortified microsomes, incubations containing the acyl glucuronide produced additional metabolites (third panel in Figs. 6 and 9). Were hydrolysis to parent compound and subsequent oxidation to take place, it would be expected that the profiles should be nearly identical

and, quite clearly, they were not. On the other hand, the presence of several aglycones, including M3, M4, M6, M12, M14 and M15 indicate that the acyl glucuronide underwent hydrolysis after it was oxidized. Differences in the chemical and enzymatic hydrolytic stability of acyl glucuronides have been well-documented (Spahn et al. 1989; Bailey and Dickinson, 2003). Thus, these data confirmed that the acyl glucuronide of MRL-C was subject to oxidative metabolism. This conclusion was supported further by data showing that the oxidative metabolism of the acyl glucuronide in human liver microsomes was catalyzed by a different CYP isozyme, namely CYP2C8, rather CYP2C9, which has been shown previously to be responsible for the in vitro metabolism of MRL-C (Reed et al., unpublished observations). To our knowledge, there is only one other report in the literature on the oxidative metabolism of an acyl glucuronide, namely that of diclofenac (Kumar et al., 2002). Interestingly, like the acyl glucuronide of MRL-C, the diclofenac acyl glucuronide is also subject to hydroxylation by CYP2C8, while diclofenac itself, is hydroxylated by CYP2C9 and CYP3A4. This finding is consistent with reports that the active site of CYP2C8 is larger and more polar than that of CYP2C9 (Schoch et al., 2004; Tanaka et al., 2004).

In conclusion, the acyl glucuronide of MRL-C was shown to undergo oxidative metabolism to a much greater extent in monkey preparations than in those from dogs, humans and rats, in that order. It is possible that this phenomenon contributed to the species differences in the in vivo elimination of MRL-C. The data showed that both Phase I and Phase II metabolism were important metabolic reactions in monkeys, while Phase II metabolism was predominant in rats and dogs. From the data generated in this

study, it would be expected that pattern of elimination of MRL-C in humans would be similar to that in dogs and rats rather than in monkeys.

ACKNOWLEDGMENTS

We thank the following people, all of Merck Research Laboratories: M. Braun, Y. Zhao, D. Dean, and A. Jones for synthesis and purification of [^{14}C] MRL-C; M. Shou and T. Rushmore for providing anti-CYP monoclonal antibodies; C. Freeden, R. Alvaro, J. Pang, and Z. Chen for help with the animal studies and processing of some of the samples; B. Karanam, M.-S. Kim, and S. H. L. Chiu for many valuable discussions. Also, we would like to acknowledge the contribution of Paul Zavorskas and other personnel of the Charles River Laboratories in the studies involving dogs and monkeys.

REFERENCES

Bailey MJ and Dickinson RG (2003) Acyl glucuronide reactivity in perspective: biological consequences. *Chem Biol Interact* **145**: 117-37.

Berger J, and Moller DE, (2002) The mechanisms of action of PPARs. *Ann Rev Med* **53**: 409-435.

Bishop-Bailey D (2000) Peroxisome proliferator-activated receptors in the cardiovascular system. *Brit J Pharmacol* **129**: 823-834.

Kersten S, Desvergne B, and Wahli W, (2000) Roles of PPARs in health and disease. *Nature* **405**: 421-424.

Kumar S, Samuel K, Subramanian R, Braun MP, Stearns RA, Chiu S-HL, Evans DC, Baillie TA, (2002) Extrapolation of diclofenac clearance from in vitro microsomal metabolism data: role of acyl glucuronidation and sequential oxidative metabolism of the acyl glucuronide. *J Pharmacol Exp Therap* **303**: 969-978.

Liu K, Xu L, Berger JP, MacNaul KL, Zhou G, Doebber TW, Forrest MJ, Moller DE, and Jones AB, (2005). Discovery of a novel series of Peroxisome proliferator-activated receptor α/γ dual agonists for the treatment of type-2 diabetes and dyslipidemia. *J Med Chem* **48:** 2262-2265.

Mei Q, Tang C, Assang C, Lin Y, Slaughter D, Rodrigues AD, Baillie TA, Rushmore TH, and Shou M, (1999) Role of a potent inhibitory monoclonal antibody to cytochrome P-450 3A4 in assessment of human drug metabolism. *J Pharmacol Exp Therap* **291**: 749-759.

Pang JM, Zaleski J, and Kauffman FC (1997) Toxicity of allyl alcohol in primary cultures of freshly isolated and cryopreserved hepatocytes maintained on hydrated collagen gels. *Toxicol Appl Pharmacol* **142**: 87-94.

Parkinson A, (1996) Biotransformation of Xenobiotics, in *Casarett & Doull's Toxicology: The Basic Science of Poisons* (Klaassen CD, ed.) pp. 113-186, McGraw-Hill.

Raucy JL and Lasker JM (1991) Isolation of P450 enzymes from human liver. *Methods Enzymol* **206**:577-587.

Rushmore TH, Reider PJ, Slaughter D, Assang C, and Shou M (2000) Bioreactor systems in drug metabolism: synthesis of cytochrome P450-generated metabolites. *Metab Eng* **2**: 115-125.

Schoch GA, Yano JK, Wester MR, Griffin KJ, Stout CD, Johnson EF (2004) Structure of human microsomal cytochrome P450 2C8. Evidence for a peripheral fatty acid binding site. *J Biol Chem* **279**: 9497-9503.

Schoonjans K, Staels B, and Auwerx J, (1996) The peroxisome proliferator activated receptors (PPARs) and their effects on lipid metabolism and adipocyte differentiation. *Biochim Biophys Acta* **1302**: 93-109.

Spahn H, Iwakawa S, Lin ET, and Benet LZ, (1989) Procedures to characterize in vivo and in vitro enantioselective glucuronidation properly: studies with benoxaprofen glucuronides. *Pharm Res* **6**: 125-132.

Tanaka T, Kamiguchi N, Okuda T, Yamamoto Y, (2004) Characterization of the CYP2C8 active site by homology modeling. *Chem Pharm Bull (Tokyo).* **52**: 836-841.

Wahli W, Braissant O, and Desvergne B, (1995) Peroxisome proliferator activated receptors: Transcriptional regulators of adipogenesis, lipid metabolism and more. *Chem Biol* **2**: 261-266.

Wang PP, Beaune P, Kaminsky LS, Dannan GA, Kadlubar FF, Larrey D, and Guengerich FP, (1983) Purification and characterization of six cytochrome P450 isozymes from human liver microsomes. *Biochemistry* **22**: 5375-5383.

Willson TM, Lambert MH, and Kliewer SA, (2001) Peroxisome proliferator-activated receptor gamma and metabolic disease. *Annu Rev Biochem* **70**: 341-367.

LEGENDS FOR FIGURES

Fig. 1. Negative ESI product ion spectrum of MRL-C. Product ion scan acquired using PE SCIEX API 3000 mass spectrometer equipped with a Turbo ion-spray source operated in the negative ion mode at 400°C.

Fig. 2. In vitro and in vivo metabolites of [^{14}C]MRL-C.

Fig. 3. Metabolite profiles for [^{14}C]MRL-C in monkey, dog, and rat bile following oral administration at 2 mg/kg. Metabolite profiles acquired using PE SCIEX API 3000 mass spectrometer (MS/MS) equipped with a Turbo ion-spray source, operated in the negative ion mode, and a PE Flow Scintillation Analyzer. Metabolites were identified by using either a constant neutral loss scan of 86 Da (loss of 2-methyl propionic acid) as the survey scan to trigger the collection of product ion spectra or multiple reaction monitoring of the major transitions for metabolites.

Fig. 4. Metabolite profiles for [^{14}C]MRL-C in monkey urine following oral administration at 2 mg/kg. Metabolite profiles acquired using PE SCIEX API 3000 mass spectrometer (MS/MS) equipped with a Turbo ion-spray source, operated in the negative ion mode, and a PE Flow Scintillation Analyzer. Metabolites were identified by using either a constant neutral loss scan of 86 Da (loss of 2-methyl propionic acid) as the survey scan to trigger the collection of product ion spectra or multiple reaction monitoring of the major transitions for metabolites.

Fig. 5. Reconstructed ion chromatogram of [^{14}C]MRL-C and metabolites in monkey bile following oral administration at 2 mg/kg. Acquired using PE SCIEX API 3000 mass spectrometer (MS/MS) equipped with a Turbo ion-spray source operated in the negative ion mode with multiple reaction monitoring of the major transitions for metabolites.

Fig. 6. HPLC Radiochromatograms of incubations of [^{14}C]MRL-C with rat, dog, monkey, and human NADPH-fortified liver microsomes. All incubations were carried out at 37°C in 0.1 M potassium phosphate at pH 7.4 in the presence of 1 mM $MgCl_2$ and 1 mg/ml protein. NADPH was added either as a freshly prepared solution in water (1 mM) or as a regenerating system consisting of 10 mM glucose-6-phosphate, 1.4 units/ml of glucose-6-phosphate dehydrogenase, and 1 mM NADP.

Fig. 7. Radiochromatograms of incubations of [^{14}C]MRL-C with rat, dog, monkey, and human NADPH- and UDPGA-fortified liver microsomes. All incubations were carried out at 37°C in 0.1 M potassium phosphate at pH 7.4 in the presence of 1 mM $MgCl_2$, 1 mg/ml microsomal protein, 50 μg/ml of alamethicin, 5 mM saccharo-1,4-lactone, and 5 mM UDPGA. NADPH was added either as a freshly prepared solution in water (1 mM) or as a regenerating system consisting of 10 mM glucose-6-phosphate, 1.4 units/ml of glucose-6-phosphate dehydrogenase, and 1 mM NADP.

Fig. 8. Radiochromatograms of a time-dependent incubation of [^{14}C]MRL-C with NADPH- and UDPGA-fortified monkey liver microsomes. The incubation was carried out at 37°C in 0.1 M potassium phosphate at pH 7.4 in the presence of 1 mM $MgCl_2$, 1

mg/ml microsomal protein, 50 μg/ml of alamethicin, 5 mM saccharo-1,4-lactone, and 5 mM UDPGA. NADPH was added as a regenerating system consisting of 10 mM glucose-6-phosphate, 1.4 units/ml of glucose-6-phosphate dehydrogenase, and 1 mM NADP. Time points were taken at 0, 5, 10, 15, 20, 30, 45, and 132 min.

Fig. 9. Radiochromatograms of incubations of [^{14}C]-labeled acyl glucuronide of MRL-C with rat, dog, monkey, and human NADPH-fortified liver microsomes. All incubations were carried out at 37°C in 0.1 M potassium phosphate at pH 7.4 in the presence of 1 mM $MgCl_2$, and 1mg/ml microsomal protein. NADPH was added either as a freshly prepared solution in water (1 mM) or as a regenerating system consisting of 10 mM glucose-6-phosphate, 1.4 units/ml of glucose-6-phosphate dehydrogenase, and 1 mM NADP.

TABLE 1

Recovery of radioactivity in bile, urine, and feces following oral and intravenous administration of [^{14}C] MRL-C to male rats, dogs, and monkeys

Species	**Dose**	**Percent of Radioactive Dose**[a]			
		Bile	**Urine**	**Feces**	**Total**[b]
Rat	2 mg/kg p.o. n = 2	96	0.2	n.d.[c]	96
	1 mg/kg i.v. n = 3	97 ± 10	0.8 ± 0.5	n.d.[c]	98 ± 10
Dog	2 mg/kg p.o. n = 3	87 ± 2	2.0 ± 0.2	5.7 ± 2.4	93 ± 4
	0.5 mg/kg i.v. n = 3	89 ± 5	2.6 ± 1.6	3.0 ± 3.4	95 ± 3
Monkey	2 mg/kg p.o. n = 2	27	42	12	88
	0.5 mg/kg i.v. n = 2	64	24	4.7	94

[a] [^{14}C] MRL-C was administered to adult, male bile duct-cannulated animals at the doses indicated. Collection periods were 0 to 72 hr (rats) and 0 to 120 hr (dogs and monkeys). Dosing vehicles and the volume administered may be found in the Materials and Methods section. Mean ± standard deviation (n=3) or average (n=2) values are listed.

[b] Total values include cage washes and cage wipes.

[c] n.d. = not determined.

TABLE 2

Metabolism of [^{14}C]MRL-C and its acyl glucuronide in liver microsomes [a]

		% Metabolism			
Compound	**Cofactor**	**Rat**	**Dog**	**Monkey**	**Human**
MRL-C	NADPH	20	60	80	43
MRL-C	UDPGA	74	67	84	76
MRL-C[b]	NADPH and UDPGA	78	83	94	88
Acyl glucuronide	NADPH	6	34	73	17

[a] Incubations were carried out at 37° for 30 min with 1 mg protein/ml, 10 μM substrate, 5 mM saccharo-1,4-lactone (no saccharolactone for MRL-C with NADPH-only incubation), and 1 mM $MgCl_2$ in 0.1 M phosphate, pH 7.4 C. Final concentrations of NADPH and UDPGA were 1 and 5 mM, respectively. The values listed were obtained from single incubations.

[b] The acyl glucuronide represented ~85, 70, 35 and 65% of total metabolism in incubations with rat, dog, monkey and human liver microsomes, respectively.

TABLE 3

Metabolism of [^{14}C]MRL-C in UGT Supersomes® [a]

UGT Supersome®	Glucuronidation (%)
1A1	<1
1A3	9
1A4	1
1A6	0
1A8	<1
1A9	12
1A10	<1
2B7	37
2B15	<1

[a] Incubations were carried out at 37° for 30 min with 0.5 mg protein/ml, 10 μM substrate, 5 mM saccharo-1,4-lactone, 5 mM UDPGA and 1 mM $MgCl_2$ in 0.1 M phosphate, pH 7.4 C. The values listed were obtained from single incubations.

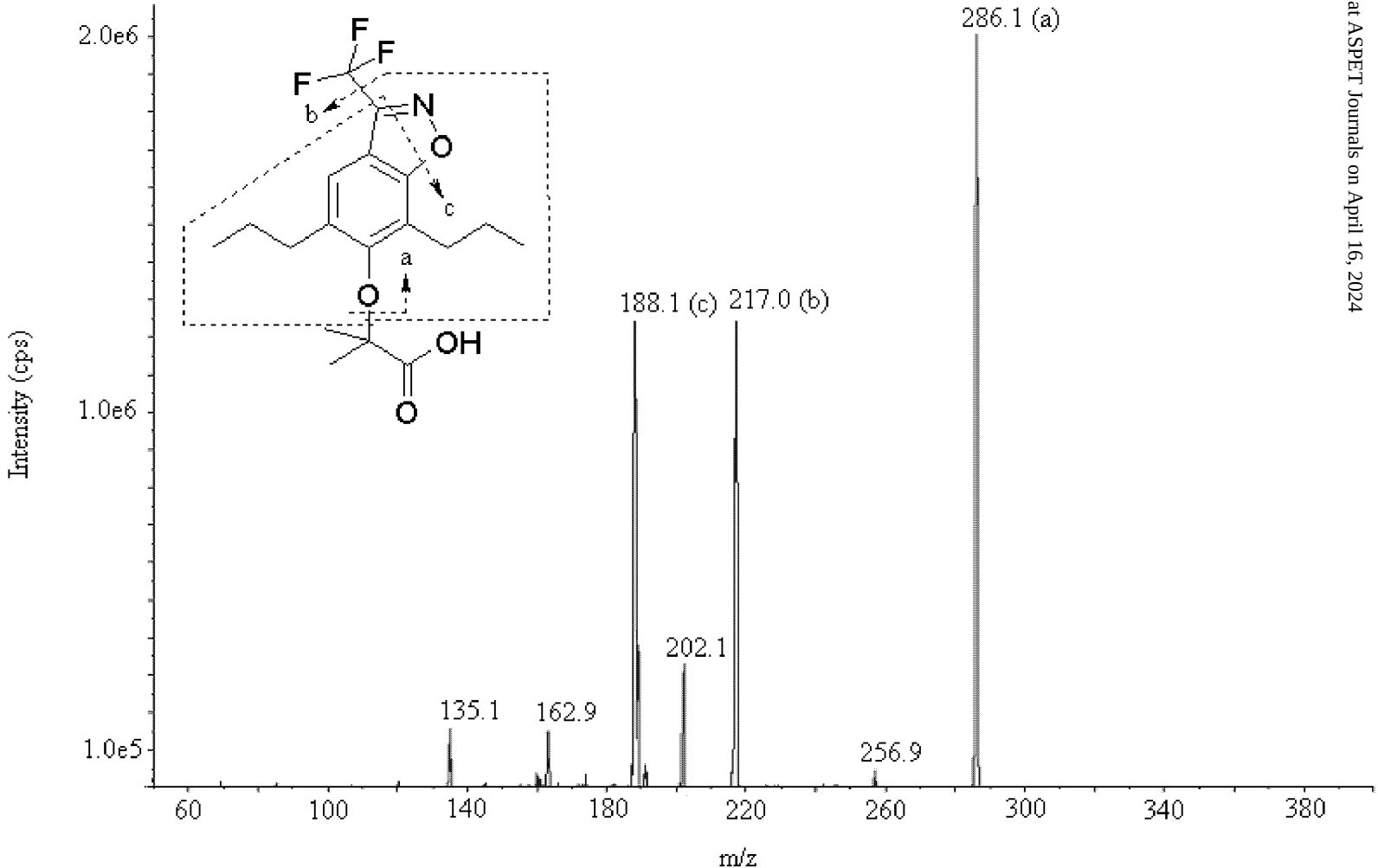

DMD Fast Forward. Published on September 23, 2005 as DOI: 10.1124/dmd.105.004010
This article has not been copyedited and formatted. The final version may differ from this version.

Fig.2

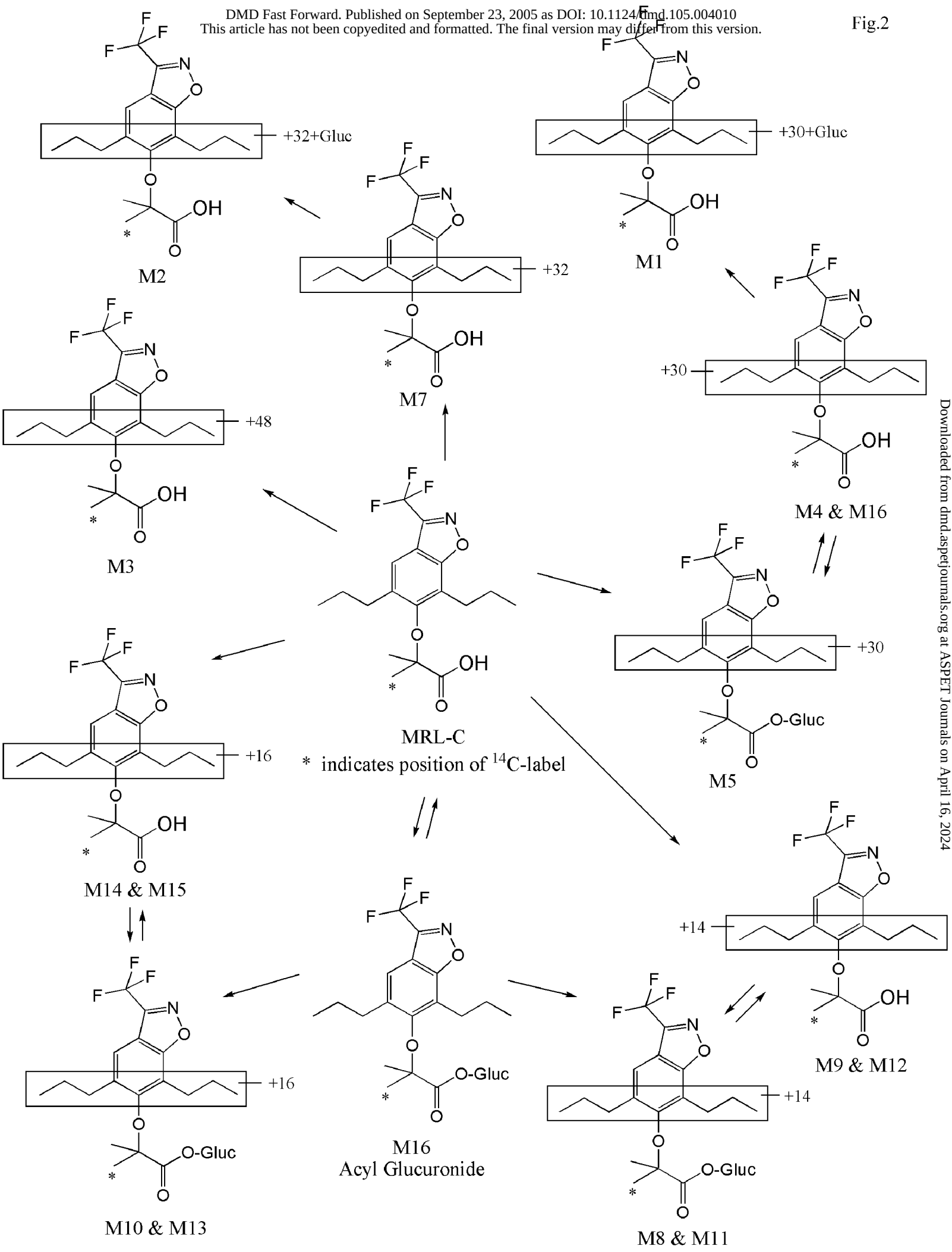

Fig.3

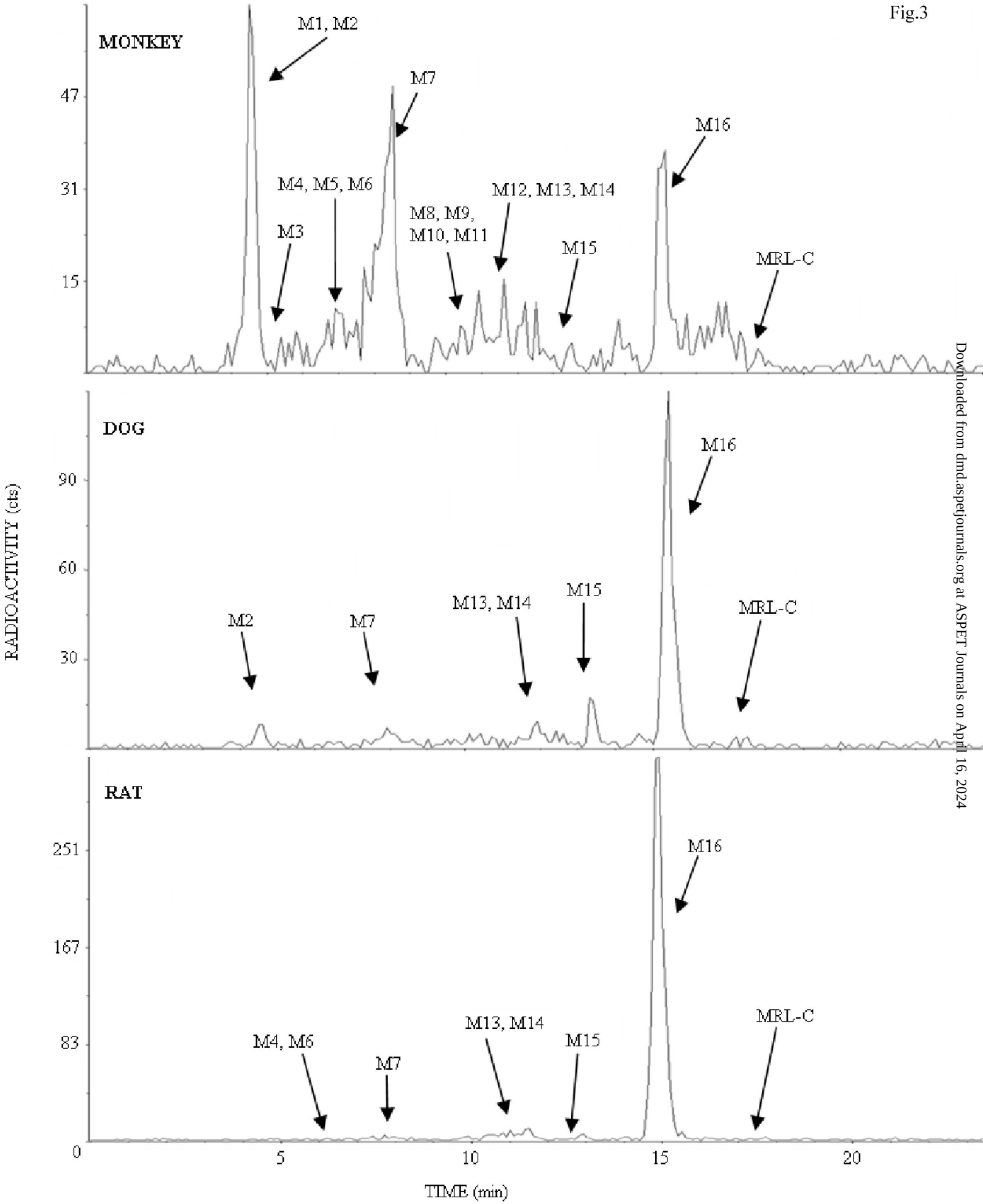

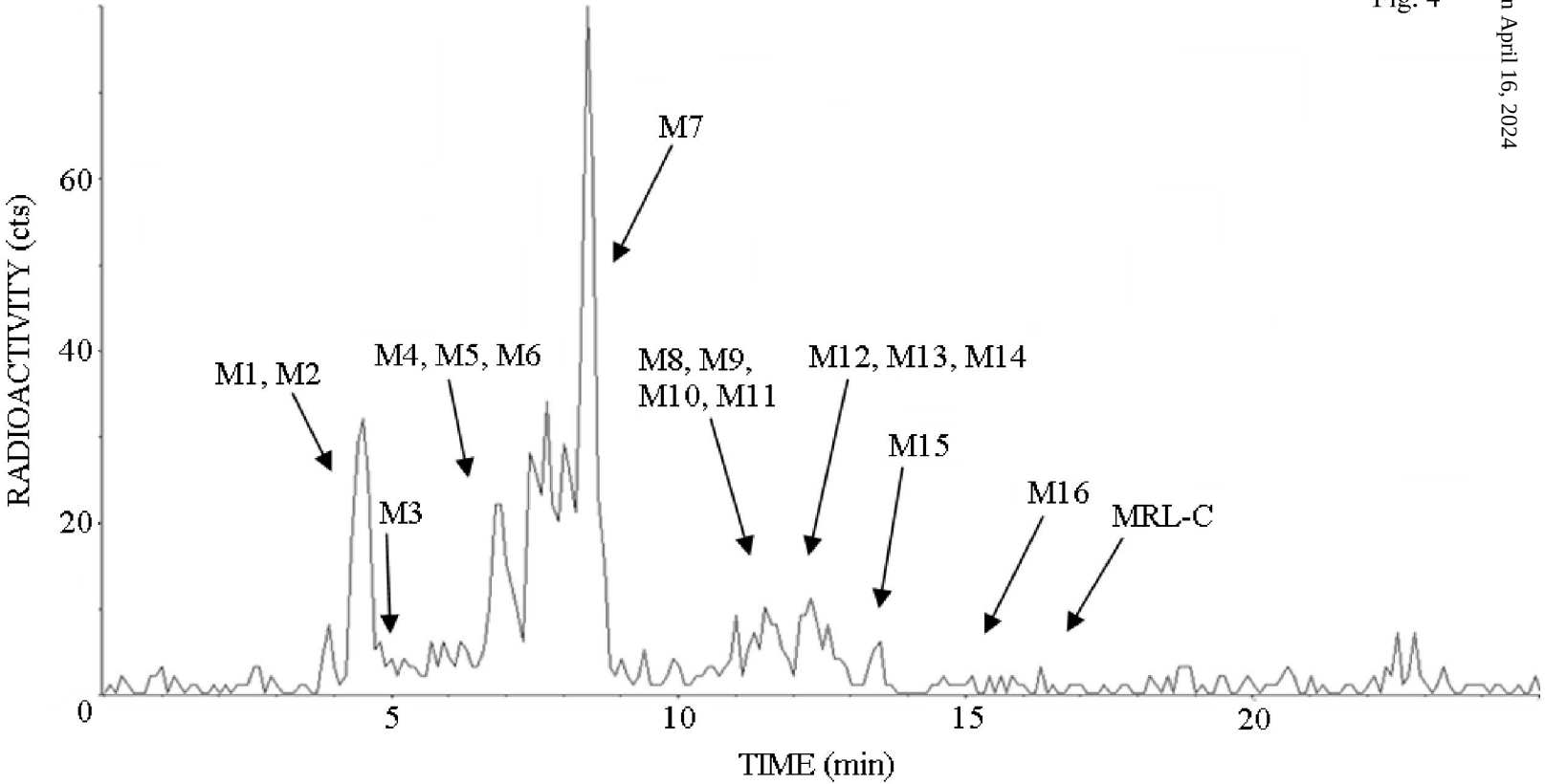

Fig.5

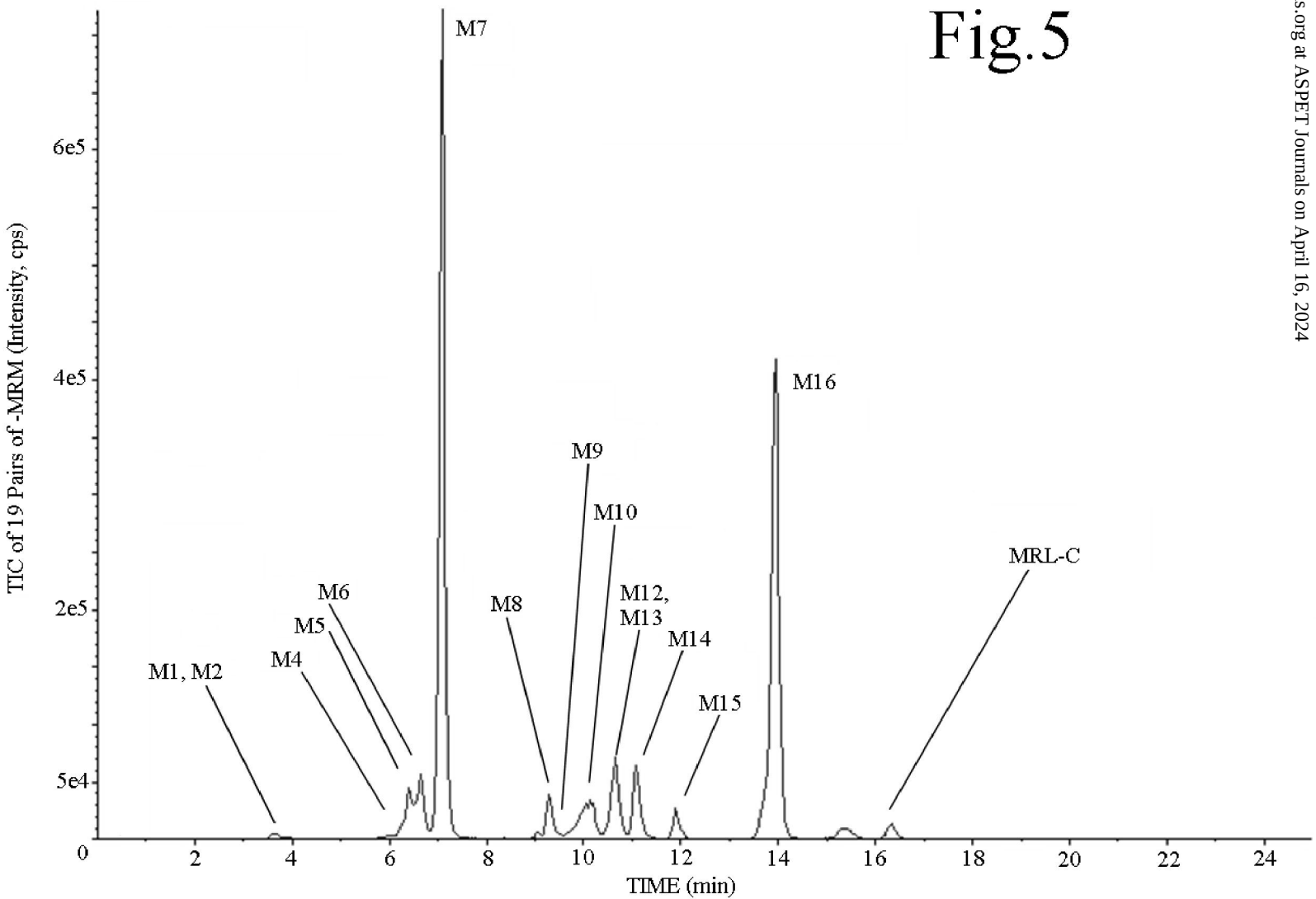

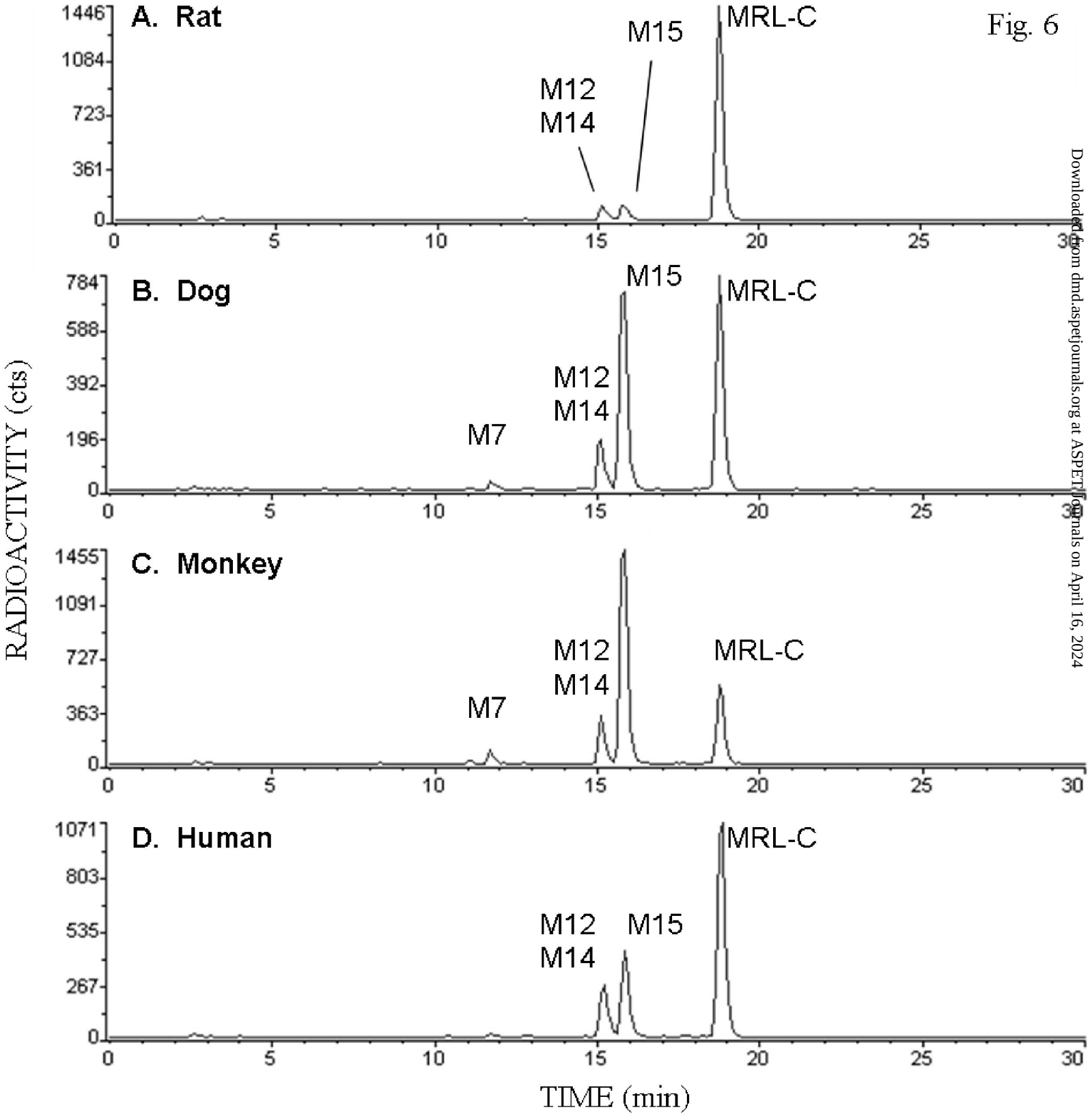

Fig. 6

Fig.7

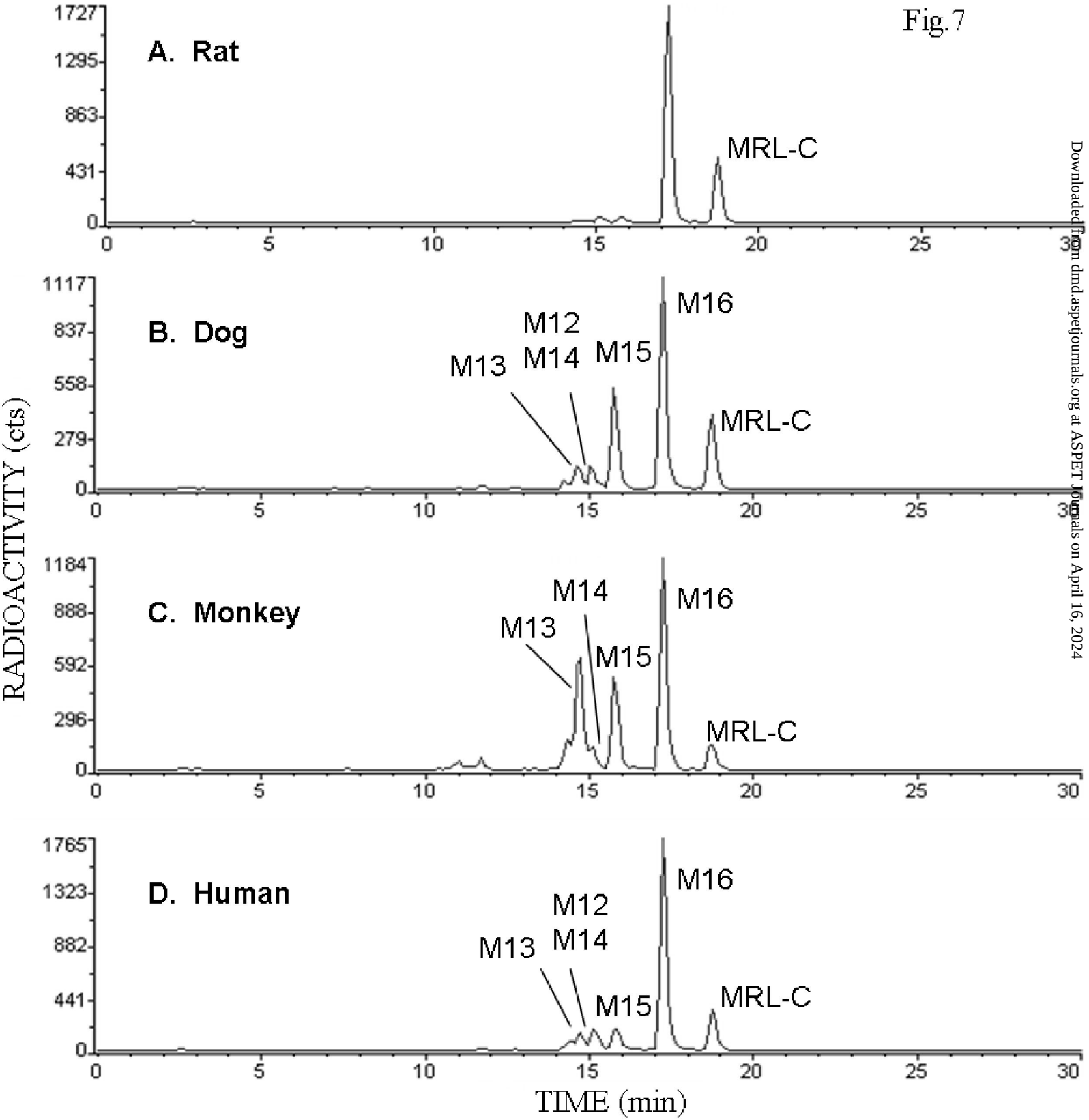

Fig.8

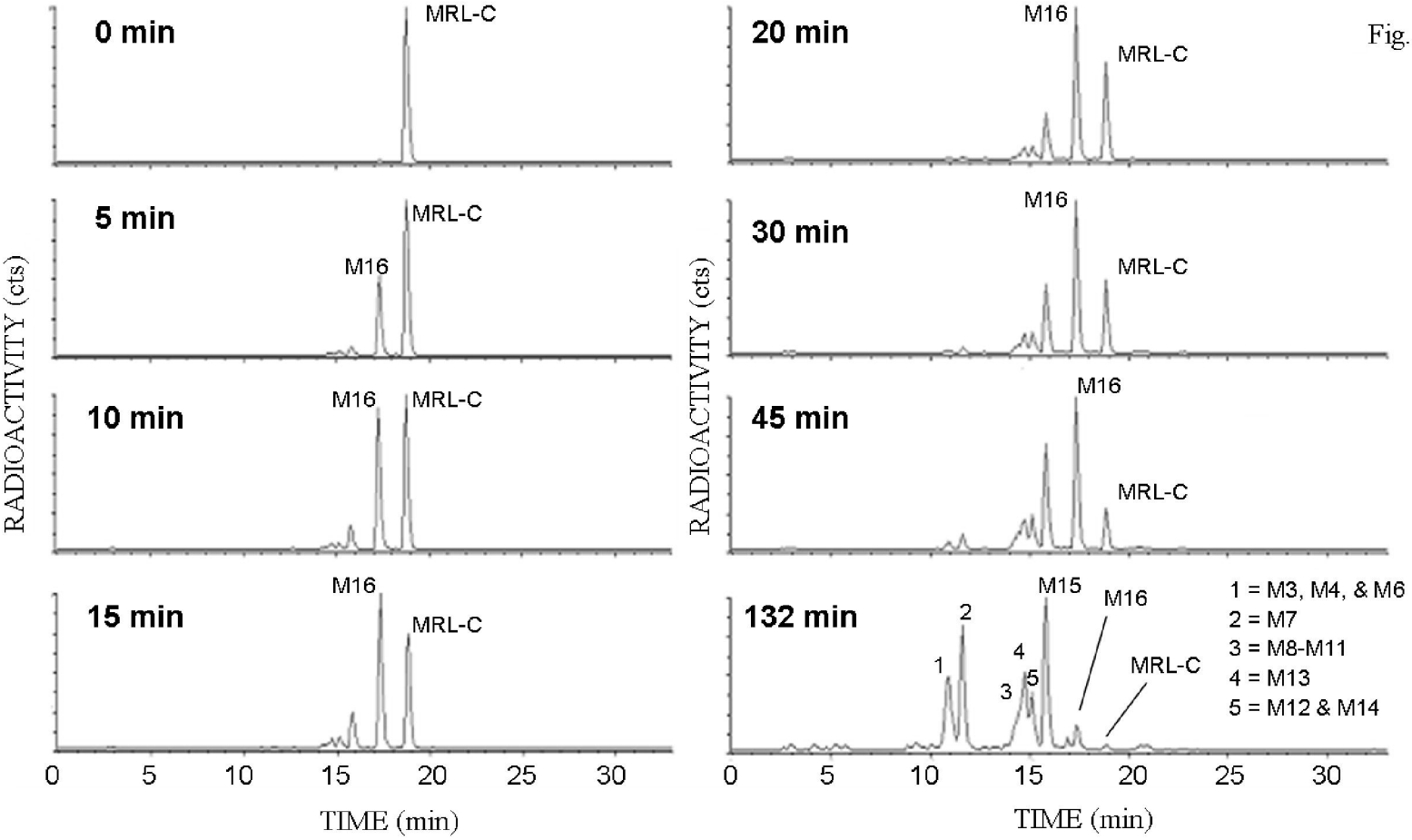

Fig.9